# Spatial investigation of the elemental distribution in Wilson´s disease liver after D-penicillamine treatment by LA-ICP-MS

Oliver Hachmöller[a,*], Andree Zibert[b,*], Hans Zischka[c], Michael Sperling[a,d], Sara Reinartz Groba[b], Inga Grünewald[e], Eva Wardelmann[e], Hartmut H.-J. Schmidt[b], and Uwe Karst[a,+]

[a] Institute of Inorganic and Analytical Chemistry, University of Münster, Corrensstraße 30, 48149 Münster, Germany

[b] Experimental Transplant Hepatology, University Hospital Münster, Albert-Schweitzer-Straße 1, 48149 Münster, Germany

[c] Institute of Molecular Toxicology and Pharmacology, Helmholtz Center Munich, Ingolstädter Landstraße 1, 85764 Neuherberg, Germany.

[d] European Virtual Institute for Speciation Analysis (EVISA), Mendelstraße 11, 48149 Münster, Germany

[e] Department of Pathology, University Hospital Münster, Domagkstraße 17, 48149 Münster, Germany

* Equal contribution

[+] Correspondence: Uwe Karst, uk@uni-muenster.de, telephone +49 251 / 83-33141, fax +49 251/83-36013

**Abstract**

At present, the copper chelator D-penicillamine (DPA) is the first-line therapy of Wilson´s disease (WD), which is characterized by an excessive copper overload. Lifelong DPA treatments aim to reduce the amount of detrimental excess copper. Although DPA shows beneficial effect in many patients, it may cause severe adverse effects. Despite several years of copper chelation therapy, discontinuation of DPA therapy can be linked to a rapidly progressing liver failure, indicating a high residual liver copper load. A high resolution (spotsize of 10 µm) laser ablation-inductively coupled plasma-mass spectrometry (LA-ICP-MS) method was applied to study the spatial distribution of copper, iron, and zinc in rat and human liver samples after DPA treatment. Untreated $LPP^{-/-}$ rats, an established animal model for WD, appeared with a high overall copper concentration and a copper distribution of hotspots distributed over the liver tissue. In contrast, a low (> 2-fold decreased) overall copper concentration was detected in liver of DPA treated animals. Importantly, however, copper distribution was highly inhomogeneous with lowest concentrations in direct proximity to blood vessels, as observed using novel zonal analysis. A human liver needle biopsy of a DPA treated WD patient substantiated the finding of an inhomogeneous copper deposition upon chelation therapy. In contrast, comparatively homogenous distributions of zinc and iron were observed. Our study indicates that a high resolution LA-ICP-MS analysis of liver samples is excellently suited to follow efficacy of chelator therapy in WD patients.

**Keywords**

- Wilson´s disease
- Elemental bioimaging
- Copper
- D-penicillamine
- Laser ablation-inductively coupled plasma-mass spectrometry (LA-ICP-MS)
- Zonal analysis

**Abbreviations**

| | |
|---|---|
| AAS | Atomic absorption spectroscopy |
| DPA | D-penicillamine |
| HE | Haematoxylin/eosin |
| LA-ICP-MS | Laser ablation-inductively coupled plasma-mass spectrometry |
| WD | Wilson´s disease |

## 1. Introduction

Wilson´s disease (WD) is a rare autosomal-recessive inherited disease of the copper metabolism leading to a copper accumulation especially in the liver and the central nervous system.[1] WD is caused by the defective gene *ATP7B*, which encodes for a metal-transporting ATPase, responsible for the biliary excretion of excess copper.[2, 3] The diagnosis of WD is complex due to manifold hepatic and neuropsychiatric symptoms as well as high variability of laboratory results.[4, 5]

A lifelong and continuous therapy is required for WD in order to maintain the copper homeostasis, allowing for a normal life expectancy in many WD patients.[6] Currently, copper chelating agents like D-penicillamine (DPA) and trientine, zinc salts, or a combination thereof are clinically applied for WD therapy.[5] Chelating agents are typically employed in order to remove excess copper from the organism and to cause a negative copper balance.[5] Zinc salts can be applied to induce metallothionein in the gastrointestinal tract and in hepatocytes, which shows a high affinity for copper due to a cysteine-rich structure.[7, 8] If a conventional therapy with chelating agents is not effective or a fulminant form of WD occurs, a liver transplantation becomes mandatory.[9]

DPA treatment, which was first used in 1956, is the first-line therapy for WD.[5, 10] However, DPA may cause severe adverse effects and even worsening of neurological symptoms in WD patients.[11] Furthermore, upon discontinuation of the DPA treatment, a rapid clinical deterioration may take place, resulting in the necessity of a liver transplantation or even in the death of the patient.[12] This rapidly deteriorating liver status has been suggested to be the result of insufficient copper elimination by DPA in WD patient livers. In fact, massively elevated liver copper levels have been reported in WD patients despite decades of DPA therapy.[13]

To investigate the distribution of remaining copper, spatially resolved techniques for elemental bioimaging such as laser ablation-inductively coupled plasma-mass spectrometry (LA-ICP-MS) offer outstanding characteristics to detect copper within the liver tissue. LA-ICP-MS was first applied for elemental bioimaging in 1994 by Wang et al. and exhibits a high spatial resolution in a micrometer range as well as limits of detection in the µg/kg range.[14, 15, 16] Additionally, analyte quantification is possible by internal and external calibration.[17] In the literature, different examples for elemental bioimaging in rat, sheep, and human liver tissues are described.[18, 19, 20, 21, 22] A recent study for the investigation of rat and human liver by LA-ICP-MS was published by Boaru et al. using a spatial resolution of 60 µm and an external calibration with matrix-matched standards made of mouse brain. This work focused especially on total elemental concentrations showing an age-dependent accumulation of copper, iron, and zinc in *Atp7b* deficient mice as well as an elevation of these metals in human WD liver. Although regions with elevated elemental concentrations within the rat and human liver samples were detected, no information on smaller structures within the liver tissue has been discussed due to the relatively low resolution of 60 µm in this study.[21]

In the present study, LA-ICP-MS is used for high resolution elemental bioimaging of copper, iron, and zinc in livers of a DPA treated WD patient and a WD animal model, the LPP$^{-/-}$ rat. The presented LA-ICP-MS method offers a spatial resolution of 10 µm spotsize and allows for quantification of physiological copper, iron, and zinc concentrations in liver tissue. Additionally, these elements are quantified by external calibration with matrix-matched gelatine standards. A sample set including LPP rat liver samples with and without DPA treatment is analyzed. *Atp7b*$^{-/-}$ deficient LPP$^{-/-}$ rats with and without several weeks of DPA treatment are compared to unaffected LPP$^{+/-}$ controls. Next to the determination of the total elemental concentrations in these rat

liver samples, the small spotsize of 10 µm offers a spatial resolution sufficient for elucidation of a copper wash-out in proximity of blood vessels upon DPA therapy. A zonal analysis is performed to depict the copper concentrations with respect to the distance to blood vessels in order to evaluate the copper concentration and distribution within the liver tissue. In addition to this, a human liver sample from a DPA treated WD patient has been analyzed by LA-ICP-MS.

## 2. Experimental

### 2.1. Chemicals and reagents

All chemicals were used in the highest quality available. Copper (II) sulfate pentahydrate, iron (III) chloride, zinc (II) chloride, multi-elemental standard IV (1000 mg/L), nitric acid (65%, Suprapur), ethanol, and xylene were obtained from Merck KGaA (Darmstadt, Germany). Rhodium and gallium standard solutions (each 1000 mg/L) were purchased from SCP Science (Baie D´Urfé, Canada). Gelatine was obtained from Grüssing GmbH (Filsum, Germany). All solutions were prepared with doubly distilled water generated by an Aquatron Water Still purification system model A4000D (Barloworld Scientific, Nemours Cedex, France).

### 2.2. Liver sample preparation

The LPP rat strain was housed and treated with DPA as described elsewhere.[23] After sacrifice of the animals, a part of the liver was used for bulk analysis by means of atomic absorption spectroscopy (AAS) and the other part of the liver was embedded in paraffin for histopathology and analysis by means of LA-ICP-MS. Areas in proximity of blood vessels of each rat liver sample with a size of 1500 x 1500 $\mu m^2$ were selected for analysis by means of LA-ICP-MS.

The investigation of the human liver sample H1 was conducted according to the Declaration of Helsinki on biomedical research involving human subjects. Formalin-fixed and paraffin-embedded (FFPE) material was obtained from the archive. Sample H1 was collected by a needle biopsy from a patient showing typical WD symptoms and following DPA treatment within a medical investigation.

Haematoxylin/eosin (HE) and rhodanine stains as well as AST and bilirubin determinations were performed according to routinely established procedures. Prior to the analysis by means of LA-ICP-MS, tissue sections of 10 µm thickness were prepared and deparaffinized by washing with xylene, ethanol, and water. Additionally, micro-

scopic images of the thin sections were captured with a BZ-9000 inverted fluorescence/bright field microscope (Keyence, Osaka, Japan).

### 2.3. Preparation of matrix-matched calibration standards

Copper, iron, and zinc within the liver samples were quantified using external calibration with matrix-matched standards made of 10% gelatine (w/w) in aqueous standard solution. The respective standard solutions were prepared by dilution of stock solutions of each element with a concentration of 10,000 $\mu g \cdot g^{-1}$, which were prepared by dissolution of iron (III) chloride, copper (II) sulfate pentahydrate, and zinc (II) chloride in doubly-distilled water. After addition of the aqueous standard solution to the gelatine, the mixture was homogenized and heated to 45°C. Standards for the different elements were prepared separately to avoid a denaturation of the gelatine and to ensure a homogeneous analyte distribution within the standards. The following concentration ranges were covered by five calibration points for each calibration function: 10 to 500 $\mu g \cdot g^{-1}$ for iron, 50 to 1000 $\mu g \cdot g^{-1}$ for copper, and 5 to 200 $\mu g \cdot g^{-1}$ for zinc. Preparation of standards with very high metal concentrations was limited due to denaturation of the gelatine that occurred for example at iron concentrations higher than 500 $\mu g \cdot g^{-1}$. According to the thickness of the liver sample sections, the gelatine standards were sectioned at 10 µm using a cryotome (Cryostar, Thermo Fisher Scientific, Bremen, Germany).

For validation purposes, the bulk copper, iron, and zinc concentrations of the gelatine standards were determined by ICP-MS. Precisely 100 mg of the respective standard material were weighed in. As internal standard, rhodium was added with a final concentration of 1 $ng \cdot g^{-1}$. In a next step, the gelatine was digested by addition of 1 mL nitric acid and the solution was filled up with doubly distilled water to 50 mL. To obtain final analyte concentrations below 30 $ng \cdot g^{-1}$, the digested standard solutions were further diluted with nitric acid (2% (w/v)). A multi-elemental ICP standard was

applied for external calibration in a concentration range from 1 to 30 ng·g$^{-1}$ covered by five calibration points.

### 2.4. Instrumentation and experimental parameters

A commercial laser ablation system LSX-213 (Teledyne CETAC Technologies, Omaha, USA) with a wavelength of 213 nm, equipped with an in-house built flat cell, was used for laser ablation experiments.[24] For detection, a quadrupole-based ICP-MS iCAP Qc (Thermo Fisher Scientific) was applied. The laser ablation system was coupled to the ICP-MS system via a Tygon® tube.

To provide a suitable spatial resolution, a spotsize of 10 µm was applied at a scan rate of 20 µm/s for the rat liver samples and for the human liver sample H1. The ablation was performed in a line by line scan with a distance of 0 µm between the ablated lines to achieve a complete ablation of the sample material. For material transport out of the ablation cell, a helium carrier gas flow of 800 mL/min was applied. Additionally, an argon gas flow of 400 mL/min was added directly after the ablation cell via a Y-piece. To monitor the plasma stability, a gallium solution (1 ng·g$^{-1}$) was introduced via a peristaltic pump and the sample introduction unit of the ICP-MS system equipped with a PFA µFlow nebulizer (Elemental Scientific, Omaha, NE, USA) and a Peltier-cooled cyclonic spray chamber (Thermo Fisher Scientific) and added to the dry aerosol. The mixed aerosol was introduced by a quartz injector pipe with an inner diameter of 3.5 mm into the ICP. To avoid interferences between $^{56}Fe^{+}$ and $^{40}Ar^{16}O^{+}$, the ICP-MS system was used in the kinetic energy discrimination (KED) mode with a helium gas flow of 4.2 mL/min. Nickel sampler and skimmer cones were used for the ICP-MS interface. For the analysis of the standards and samples by LA-ICP-MS, the following ICP-MS conditions were used: rf power, 1550 W; cooling gas flow, 14 L/min; nebulizer gas flow, 0.5 L/min; auxiliary gas flow, 0.8 L/min. The isotopes $^{55}Mn$, $^{56}Fe$, $^{63}Cu$, $^{64}Zn$ and $^{69}Ga$ were monitored with a dwell time of 0.1 s each.

The same ICP-MS system was applied for the bulk analysis of the digested gelatine standards. A SC-4-S autosampler (Elemental Scientific) was used for the sample introduction of the gelatine standards into the ICP-MS. The ICP-MS was equipped with a PFA µFlow nebulizer (Elemental Scientific), a Peltier-cooled cyclonic spray chamber (Thermo Fisher Scientific), a quartz injector pipe with an inner diameter of 1.0 mm and platinum sampler and skimmer cones. Again, the ICP-MS was used in the KED mode with a cell gas flow of 4.3 mL/min to avoid interferences. The following conditions were used for the ICP-MS system: rf power, 1550 W; cooling gas flow, 14 L/min; nebulizer gas flow, 1.1 L/min; auxiliary gas flow, 0.5 L/min. The isotopes $^{56}$Fe, $^{63}$Cu, $^{64}$Zn and $^{103}$Rh were monitored with a dwell time of 0.1 s.

**2.5. Data analysis for elemental bioimaging**

During the laser ablation experiment, a transient signal was collected, which was converted into a 2D image using Origin 8.0 (Originlab Corporations, Northampton, MA, USA) and ImageJ (National Institute of Health, Bethesda, MD, USA). Processing of the calibration data was carried out by linear calibration of the average signal intensities of the standards. The resulting calibration functions were applied to calculate the copper, iron, and zinc concentrations within the liver samples. Concentrations exceeding the upper concentration of the calibration function were determined by extrapolation.

**2.6. Zonal analysis**

To evaluate the influence of the DPA treatment on the copper distribution within the rat liver samples, a zonal analysis of the copper concentration with respect to the distance to blood vessels was carried out. For zonal analysis, blood vessels within the analyzed liver samples with an area above 500 µm$^2$ were selected. The copper concentrations within the liver tissue along 4 directions originating from the respec-

220 tive blood vessel were considered and averaged for all blood vessels of the three
221 different sample groups.

## 3. Results and discussion

### 3.1. Characteristics of the rat liver samples used for LA-ICP-MS analysis

Our strategy involved a side-to-side analysis of standard protocols routinely used in the diagnosis of WD and LA-ICP-MS analysis. The LPP$^{-/-}$ rats carry the WD-causing genotype *Atp7b*$^{-/-}$ and were either untreated or subjected to DPA treatment (Table 1).[25] Unaffected healthy rats (LPP$^{+/-}$, genotype *Atp7b*$^{+/-}$) served as a control. Liver disease markers were highly elevated in untreated LPP$^{-/-}$ rats as compared to DPA treated LPP$^{-/-}$ rats or controls as reported before.[23, 26] Haematoxylin and eosin (HE) liver stains of the untreated animals indicated lobular inflammation, ballooning, and areas of focal cell death (Supplemental figure 1). Almost normal liver parenchyma was observed in the HE stains of the two other animal groups. In figure 1, some rhodanine stained areas were observed in untreated LPP$^{-/-}$ rats, whereas copper-specific staining was almost absent in the liver sections derived from the DPA treated LPP$^{-/-}$ rats and controls. Our results confirm previous findings indicating that, while rhodanine staining can be used for detection of copper in paraffin sections of the WD liver, such histochemical analysis is variable to some extent and does not allow a high grade of quantification.[27, 28, 29]

Table 1: Liver samples and WD disease markers of the LPP rats.

| Sample | Age at sacrifice (days) | *ATP7B* Genotype | Treatment, duration (days) | AST [U/L] | Bilirubin [mg/dL] | Areas for LA-ICP-MS analysis |
|---|---|---|---|---|---|---|
| 1 | 94 | -/- | No | 790.0 | 6.95 | 5 |
| 2 | 94 | -/- | No | 1940.0 | 36.45 | 5 |
| 3 | 121 | -/- | DPA, 36 | 110.0 | <0.5 | 5 |
| 4 | 122 | -/- | DPA, 37 | 100.0 | <0.5 | 5 |
| 5 | 91 | +/- | No | 106.0 | <0.5 | 4 |
| 6 | 84 | +/- | No | 112.0 | <0.5 | 4 |

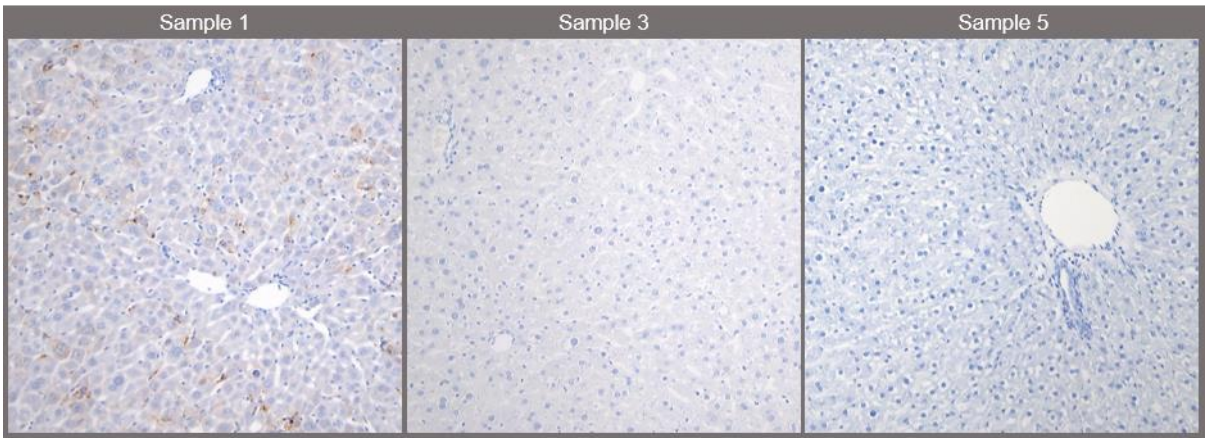


Figure 1: Brightfield microscopic images of the rhodanine stained liver tissue. As an example stains from samples 1, 3, and 5 are shown (magnification 100x).

### 3.2. Calibration by matrix-matched gelatine standards for LA-ICP-MS

For quantification of elements in paraffin-embedded liver sections by LA-ICP-MS, thin sections of the matrix-matched standards for copper, iron, and zinc were prepared with a thickness of 10 µm and ablated applying the same parameters, which were used for the analysis of the rat and human liver samples. Prior to the ablation of the sample, an area of eleven lines was ablated with a length of 600 µm for each gelatine standard. The first line of each area was not considered for calibration, while more material is ablated for the first line, because some ablation can be observed for areas outside the nominal spotsize.

The calibration functions revealed a good linearity with regression coefficients of $R^2 = 0.998$ for $^{56}Fe$, $R^2 = 0.999$ for $^{63}Cu$, and $R^2 = 0.995$ for $^{64}Zn$. Analyses of the standards showed RSDs of 9.8% and below for $^{56}Fe$, 5.1% and below for $^{63}Cu$, and 5.1% and below for $^{64}Zn$, indicating a homogeneous analyte distribution within the gelatine. Based on the 3- and 10-σ criterion, the following limits of detection and quantification were calculated for LA-ICP-MS analysis with a spotsize of 10 µm: 2.4 and 7.9 $\mu g \cdot g^{-1}$ for $^{56}Fe$, 0.3 and 1.1 $\mu g \cdot g^{-1}$ for $^{63}Cu$, and 0.7 and 2.4 $\mu g \cdot g^{-1}$ for $^{64}Zn$.

For validation purposes, the bulk copper, iron, and zinc concentrations of the matrix-matched gelatine standards were determined after digestion.

With a spotsize of 10 µm, the spatial resolution of the applied LA-ICP-MS method is suitable for the zonal analysis of the elemental distribution within the rat liver samples, while featuring limits of quantification even appropriate for the analysis of physiological concentrations in control samples.

### 3.3. Total elemental concentrations in rat liver samples by LA-ICP-MS

In order to determine the elemental concentrations in the rat liver samples by LA-ICP-MS, areas in the proximity of blood vessels with a size of 1,500 x 1,500 $\mu m^2$ were analyzed in each sample with a spot size of 10 µm. Quantification of elements was carried out with matrix-matched gelatine standards. The total concentrations of copper, iron, and zinc were calculated by averaging the local concentrations within the liver sections (Table 2). For comparison, the copper concentrations were also determined by bulk analysis using AAS, which represents the method of choice for copper determinations in the diagnosis of WD. Of note, analysis by LA-ICP-MS revealed copper concentrations that were in the same range as determined by AAS. The observed minor differences between the values derived by LA-ICP-MS and AAS are most likely due to a biological variation of the liver specimen, since only one thin section was considered for analysis by LA-ICP-MS, whereas a higher volume of the liver is analyzed by AAS. Nevertheless, our data suggest that LA-ICP-MS has a sufficiently high power of precision for the determination of the total copper concentration, while the copper concentrations of different areas of each sample analyzed by LA-ICP-MS showed a small variability.

Iron concentrations showed values in the samples ranging from 61 to 260 $\mu g \cdot g^{-1}$ (SD 63 $\mu g \cdot g^{-1}$). In the Long Evans Cinnamon (LEC) rat model of WD an increased liver iron concentration has been observed, while varying concentrations from WD pa-

tients were reported.[30, 31] No direct correlation of iron and copper values was observed in our analysis of the LPP$^{-/-}$ rats (Pearson coefficient $r < 0.5$), however, lowest iron concentrations were found in DPA treated animals suggesting that DPA might also act as an iron chelator to some extent, although the iron-DPA complex is less stable.[32] Of note, zinc concentrations were almost identical in all samples in a range from 45 to 59 $\mu g \cdot g^{-1}$ (SD 5 $\mu g \cdot g^{-1}$) indicating that zinc could be used to normalize LA-ICP-MS element determinations of liver sections.[18]

Samples obtained from untreated LPP$^{-/-}$ rats revealed strongly increased copper concentrations, as expected from the disturbed copper metabolism in the *Atp7b*$^{-/-}$ rats.[25, 26] Chelation therapy leads to decreased copper concentrations by more than a factor 2 in comparison to untreated LPP$^{-/-}$ rats, demonstrating the therapeutic efficacy of mid- to long-term DPA treatments, suggesting highly efficient copper removal from the liver tissue.[33] Due to the fact that all samples showed similar zinc concentrations, a general influence of the DPA therapy on the zinc concentration within the rat liver tissue is not observed in this study, although DPA is known to increase the urinary excretion of zinc of WD patients.[34]

Table 2: Total elemental concentrations of the LPP rat liver samples. SD of concentrations determined by LA-ICP-MS were calculated over all analyzed data points.

| Sample | c(Cu)/ $\mu g \cdot g^{-1}$ (AAS) | c(Cu)/ $\mu g \cdot g^{-1}$ (LA-ICP-MS) | c(Fe)/ $\mu g \cdot g^{-1}$ (LA-ICP-MS) | c(Zn)/ $\mu g \cdot g^{-1}$ (LA-ICP-MS) |
|---|---|---|---|---|
| 1 | 454 | 402 ± 156 | 187 ± 101 | 45 ± 11 |
| 2 | 411 | 267 ± 131 | 260 ± 137 | 59 ± 15 |
| 3 | 194 | 121 ± 35 | 61 ± 37 | 45 ± 12 |
| 4 | 172 | 192 ± 101 | 102 ± 70 | 49 ± 17 |
| 5 | 7 | 39 ± 10 | 163 ± 59 | 49 ± 12 |
| 6 | 7 | 46 ± 8 | 155 ± 69 | 45 ± 9 |

### 3.4. Quantitative elemental bioimaging of rat liver samples by LA-ICP-MS

One advantage of LA-ICP-MS is the high spatial resolution of this methodology.[16] The elemental distribution maps for copper, zinc, and iron of all analyzed areas are

shown in the supplemental part of this work (Supplemental figures 2 to 7). Three representative sections of the spatial copper distribution, observed in one area of samples 1, 3, and 5, are shown in figure 2.

Sample 1 derived from an untreated $LPP^{-/-}$ rat reveals a concentration range from 0 to 1198 $\mu g \cdot g^{-1}$ with several local hotspots (> 600 $\mu g \cdot g^{-1}$) distributed over the liver section. The copper hotspots are located both in the proximity of the blood vessel and also in areas distant to blood vessels. This distribution of copper in a WD animal model resembles a severely diseased liver parenchyma with several local apoptotic areas that harbour elevated concentrations of copper. The interpretation is supported by the HE and rhodanine stains of parallel sections (Figure 1 and supplemental figure 1). For localization of these hotspots, the high spatial resolution of the applied LA-ICP-MS method with a spot size of 10 µm is required, while a spotsize of 60 µm leads to a significant loss of details and averaging of high concentrations (data not shown).[21]

Sample 3 of a DPA treated $LPP^{-/-}$ rat shows a copper distribution in a concentration range from 13 to 227 $\mu g \cdot g^{-1}$. Importantly, the copper distribution is inhomogeneous, while the lowest copper concentrations tend to be localized in direct proximity of the blood vessels. The copper distribution map of sample 5 derived from $LPP^{+/-}$ control rat reveals a very homogeneous distribution in a concentration range from 3 to 73 $\mu g \cdot g^{-1}$. Within the analyzed area, no localization of copper in specific parts of the liver tissue could be recognized. As no genetic defect and therefore no disturbed copper metabolism is present in this animal, a homogenous copper concentration may represent the physiological state of the normal liver.

For an improved quantification of the copper distribution within the rat liver samples, a zonal analysis was performed to depict the copper concentration with respect to the distance to blood vessels. Thereto, the copper concentrations within the liver tissue

along 4 directions originating from the respective blood vessel were considered and averaged for all blood vessels of all six samples. Results of the mean copper concentrations for the three sample groups are shown in figure 3.

The samples derived from untreated $LPP^{-/-}$ rats revealed a strong increase of the copper concentration in the direct proximity to the blood vessel. Following a distance of around 40 µm to the blood vessel, the copper concentration reached a plateau of more than 400 $\mu g \cdot g^{-1}$. In contrast, samples from DPA treated $LPP^{-/-}$ rats showed a lower increase of the copper concentration with respect to the distance to blood vessels. At around 70 µm, a plateau of more than 150 $\mu g \cdot g^{-1}$ copper was observed. Thus, the copper concentration with respect to the distance to blood vessels showed a lower slope in DPA treated animals in comparison to the untreated $LPP^{-/-}$ rats. Samples from the control $LPP^{+/-}$ group displayed a constant copper concentration of about 40 $\mu g \cdot g^{-1}$ independent from the distance to blood vessels. The quantification suggests that DPA treatment leads to an enforced local decrease of the total copper within the proximity of blood vessels (< 70 µM) possibly resulting from a wash-out of chelated copper into the circulation. Thus, our results demonstrate that copper is not removed homogeneously from the liver by DPA treatment. Areas close to blood vessels are preferably copper depleted, while more distant liver areas still appear with increased copper concentrations. Such areas of local high copper may represent copper reservoirs potentially leading to severe side effects after withdrawal of DPA therapy in WD patients.[12]

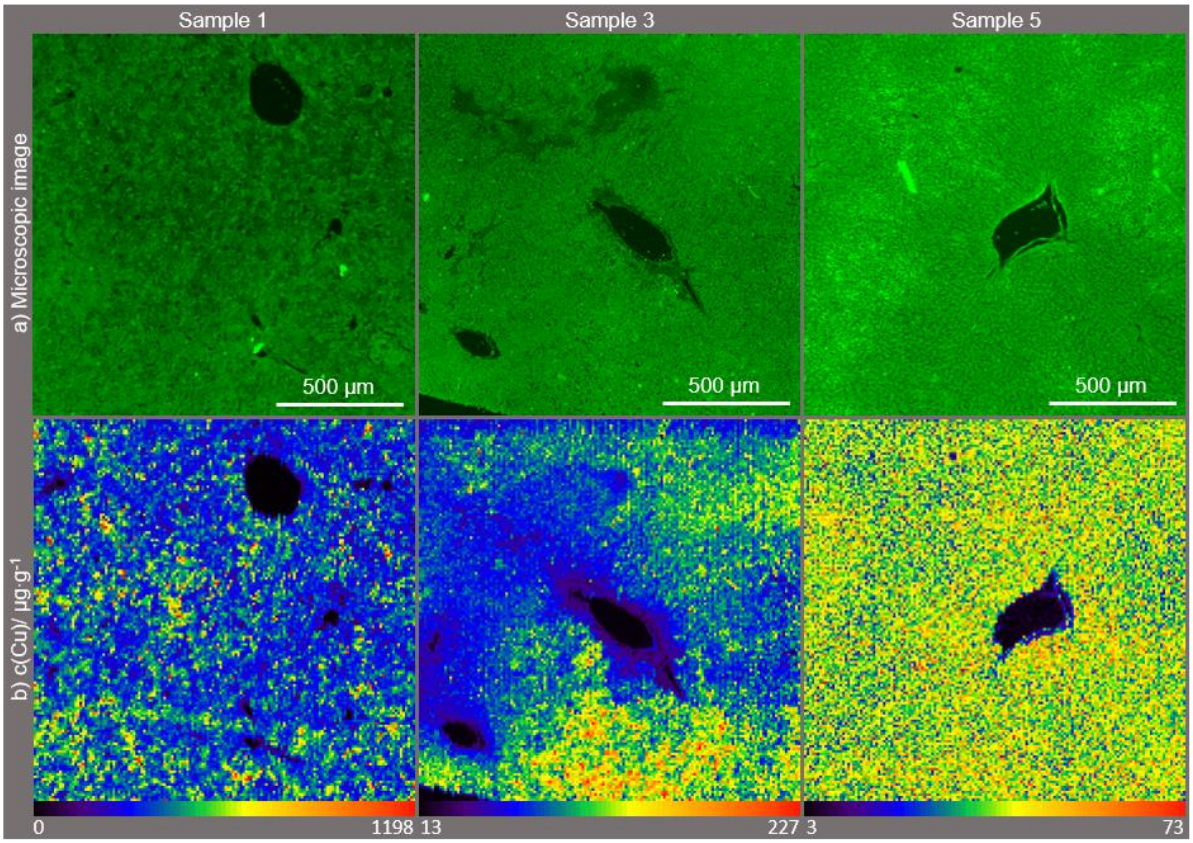


354

355 Figure 2: Autofluorescence microscopic images (a) and quantitative distribution maps of copper (b).

356 As an example distribution maps from samples 1, 3, and 5 are shown.

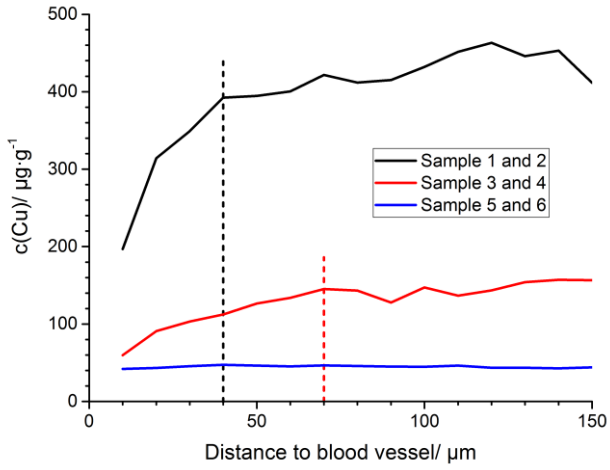


357

358 Figure 3: Zonal analysis of the copper concentration with respect to the distance to blood vessels.

359 Graphs show the results for the mean copper concentrations for the three sample groups. In total, 20

360 blood vessels were considered for sample 1 and 2, 23 for sample 3 and 4, and 12 for sample 5 and 6.

361 **3.5. Quantitative elemental bioimaging of human liver after DPA treatment by**

362 **LA-ICP-MS**

A human liver sample from a patient showing typical WD symptoms and following DPA treatment was investigated in order to study the influence of the DPA therapy on the elemental distribution.

In figure 4, the resulting distribution maps of copper and iron are shown in a concentration range from 0 to 250 $\mu g \cdot g^{-1}$ and 0 to 1000 $\mu g \cdot g^{-1}$, respectively. The total elemental concentrations of the human liver sample as determined by LA-ICP-MS was found to be at 34 $\mu g \cdot g^{-1}$, 83 $\mu g \cdot g^{-1}$, and 69 $\mu g \cdot g^{-1}$ for copper, iron, and zinc, respectively. In comparison, AAS analysis of a parallel liver biopsy taken at the same day revealed a total copper concentration of 81 $\mu g \cdot g^{-1}$.

Blood vessels were surrounded by areas with elevated copper concentrations (arrow 1) as well as by low copper concentration in direct proximity (arrow 2). Due to the small size of the needle biopsy sample, a zonal analysis of the copper distribution within the liver tissue was limited. Interestingly, the copper and iron distribution of the human sample showed an inverse correlation (Pearson coefficient $r < 0.5$) could resemble a replacement of copper by iron during long-term copper chelation due to severe hypoceruloplasminemia.[22, 31, 35] Our data indicate that human and animal liver samples show an inhomogeneous copper deposition after DPA treatment and suggest that a high resolution spatial analysis by LA-ICP-MS is highly favourable to avoid sampling errors in small biopsy samples.[22]

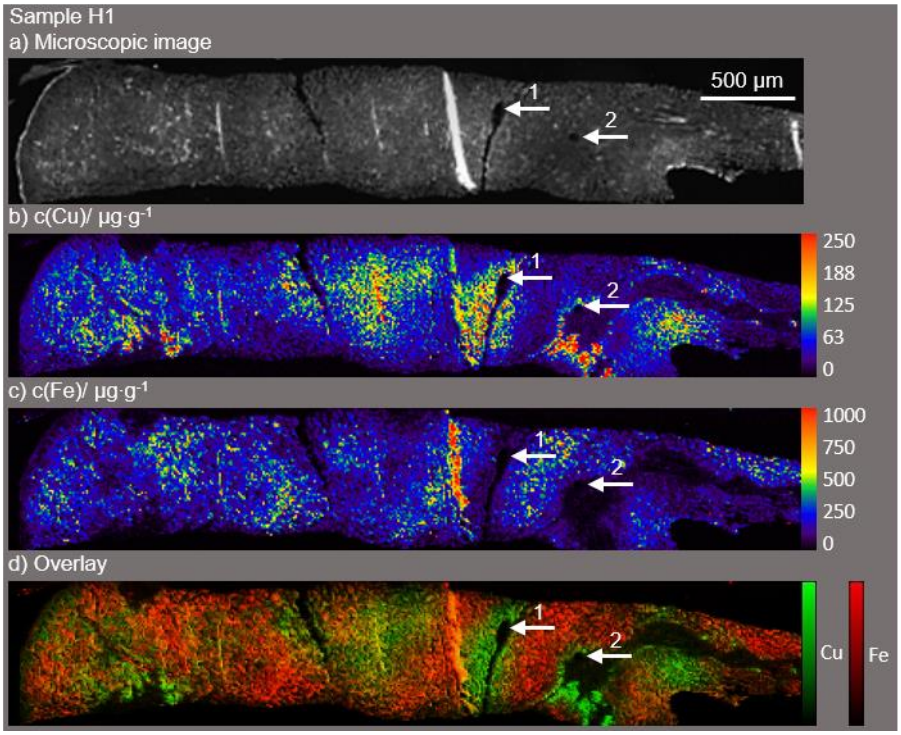


Figure 4: Autofluorescence microscopic images (a), quantitative distribution maps of copper (b) and iron (c), and overlay of the copper and iron distribution (d) of human liver sample H1 collected by a needle biopsy.

## 4. Conclusions

In this work, the suitability of LA-ICP-MS for the spatial investigation of the elemental distribution in liver samples of WD patients and a WD rat model is demonstrated. The applied LA-ICP-MS method features a spotsize of 10 µm suitable for the zonal analysis and appropriate limits of quantification for physiological element concentrations in control samples.

Results by LA-ICP-MS revealed copper hotspots distributed over the liver tissue within the diseased rat liver. The hotspots possibly resemble histological findings of high apoptotic areas. The DPA treated animals showed a significant decrease in the copper concentration by more than a factor two. However, copper distribution maps of the DPA treated animals were highly inhomogeneous and the lowest copper concentrations were localized in direct proximity to blood vessels. Furthermore, LA-ICP-MS results confirmed an inhomogeneous copper deposition in human liver tissue after DPA chelation therapy.

Taken together, our study shows that high resolution LA-ICP-MS provides very informative elemental distribution maps and therefore represents an excellent methodology to assess the efficacy of current and novel compounds used in the treatment of WD.

## 5. Acknowledgement

Parts of this study were supported by the Cells in Motion Cluster of Excellence (CiM – EXC 1003), Münster, Germany (project FF-2013-17).

## 6. References


1 A. Ala, A. P. Walker, K. Ashkan, J. S. Dooley and M. L Schilsky, *Lancet*, 2007, **369**, 397-408.

2 P. C. Bull, G. R. Thomas, J. M. Rommens, J. R. Forbes and D. W. Cox, *Nat. Genet.*, 1993, **5**, 327-337.

3 M. Y. Bartee and S. Lutsenko, *Biometals*, 2007, **20**, 627-637.

4 D. Huster, *Best Pract. Res. Clin. Gastroenterol.*, 2010, **24**, 531-539.

5 E. A. Roberts and M. L. Schilsky, *Hepatology*, 2008, **47**, 2089-2111.

6 W. Stremmel, K. W. Meyerrose, C. Niederau, H. Hefter, G. Kreuzpaintner, G. Strohmeyer, *Ann. Intern. Med.*, 1991, **115**, 720-726.

7 R. Purchase, *Sci. Prog.*, 2013, **96**, 19-32.

8 G. Chandhok, N. Schmitt, V. Sauer, A. Aggarwal, M. Bhatt and H. H.-J. Schmidt, *PLoS One*, 2014, **9**, e98809.

9 K. H. Weiss, F. Thurik, D. N. Gotthardt, M. Schäfer, U. Teufel, F. Wiegand, U. Merle, D. Ferenci-Foerster, A. Maieron, R. Stauber, H. Zoller, H. H.-J. Schmidt, U. Reuner, H. Hefter, J. M. Trocello, R. H. J. Houwen, P. Ferenci, W. Stremmel and EUROWILSON Consortium, *Clin. Gastroenterol. Hepatol.*, 2013, **11**, 1028-1035.

10 J. M. Walshe, *Lancet*, 1956, **270**, 25-26.

11 J. M. Walshe and M. Yealland, *Q. J. Med.*, 1993, **86**, 197-204.

12 I. H. Scheinberg, M. E. Jaffe and I. Sternlieb, *New Engl. J. Med.*, 1987, **317**, 209-213.

13 I. H. Scheinberg, I. Sternlieb, M. L. Schilsky and R. J. Stockert, *Lancet*, 1987, **330**, 95-95.

14 S. Wang, R. Brown and D. J. Gray, *Appl. Spectrosc.*, 1994, **48**, 1321-1325.

15 A. Sussulini and J. S. Becker, *Talanta*, 2015, **132**, 579-582.

16 J. Koch and D. Günther, *Appl. Spectrosc.*, 2011, **65**, 155a-162a.

17 D. Hare, C. Austin and P. Doble, *Analyst*, 2012, **137**, 1527-1537.

18 A. Kindness, C. N. Sekaran and J. Feldmann, *Clin. Chem.*, 2003, **49**, 1916-1923.

19 P. M-M, U. Merle, R. Weiskirchen and J. S. Becker, *Int. J. Mass. Spectrom.*, 2013, **354**, 281-287.

20 P. M-M, R. Weiskirchen, N. Gassler, A. K. Bosserhoff and J. S. Becker, *PLoS One*, 2013, **8**, e58702.

21 S. G. Boaru, U. Merle, R. Uerlings, A. Zimmermann, C. Flechtenmacher, C. Willheim, E. Eder, P. Ferenci, W. Stremmel and R. Weiskirchen, *J. Cell. Mol. Med.*, 2015, **19**, 806-814.

22 O. Hachmöller, M. Aichler, K. Schwamborn, L. Lutz, M. Werner, M. Sperling, A. Walch and U. Karst, *J. Trace Elem. Med. Bio.*, 2016, **35**, 97-102.

23 H. Zischka, J. Lichtmannegger, S. Schmitt, N. Jägemann, S. Schulz, D. Wartini, L. Jennen, C. Rust, N. Larochette, L. Galluzzi, V. Chajes, N. Bandow, V. S. Gilles, A. A. DiSpirito, I. Esposito, M. Goettlicher, K. H. Summer and G. Kroemer, *J. Clin. Invest.*, 2011, **121**, 1508-1518.

24 R. Niehaus, M. Sperling and U. Karst, *J. Anal. Atom. Spectrom.*, 2015, **30**, 2056-2065.

25 H. Zischka and J. Lichtmannegger, *Ann. N. Y. Acad. Sci.*, 2014, **1315**, 6-15.

26 J. Lichtmannegger, C. Leitzinger, R. Wimmer, S. Schmitt, S. Schulz, Y. Kabiri, C. Eberhagen, T. Rieder, D. Janik, F. Neff, B. K. Straub, P. Schirmacher, A. A. DiSpirito, N. Bandow, B. S. Baral, A. Flatley, E. Kremmer, G. Denk, F. P. Reiter, S. Hohenester, F. Eckart-Schupp, N. A. Dencher, J. Adamski, V. Sauer, C. Niemietz, H. H.-J. Schmidt, U. Merle, D. N. Gotthardt, G. Kroemer, K. H. Weiss and H. Zischka, *J. Clin. Invest.*, 2016, **126**, 2721-2735.

27 W. E. Evering, S. Haywood, M. E. Elmes, B. Jasani and J. Trafford, *J. Clin. Pathol.*, 1990, **160**, 305-312.

28 A. R. Moore, E. Coffey and D. Hamar, *Vet. Clin. Pathol.*, 2016, doi: 10.1111/vcp.12401.

29 S. Jain, P. J. Scheuer, B. Archer, S. P. Newman and S. Sherlock, *J. Clin. Pathol.*, 1978, **31**, 784-790.

30 J. Kato, Y. Kohgo, N. Sugawara, S. Katsuki, N. Shintani, K. Fujikawa, E. Miyazaki, M. Kobune, N. Takeichi and Y. Niitsu, *Jpn. J. Cancer Res.*, 1993, **84**, 219-222.

31 Y. Shiono, S. Wakusawa, H. Hayashi, T. Takikawa, M. Yano, T. Okada, H. Mabuchi, S. Kono and H. Miyajima, *Am. J. Gastroenterol.*, 2001, **96**, 3147-3151.

32 J. T. McCall, N. P. Goldstein, R. V. Randall and J. B. Gross, *Am. J. Med. Sci.*, 1967, **254**, 13-23.

33 K. Gibbs and J. M. Walshe, *J. Gastroen. Hepatol.*, 1990, **5**, 420-424.

34 M. van Caillie-Bertrand, H. J. Degenhart, H. K. A. Visser, M. Sinaasappel and J. Bouquet, *Arch. Dis. Child.*, 1985, **60**, 656-659.

35 O. Hachmöller, A. G. Buzanich, M. Aichler, M. Radtke, D. Dietrich, K. Schwamborn, L. Lutz, M. Werner, M. Sperling, A. Walch and U Karst, *Metallomics*, 2016, **8**, 648-653.